Robust Cadence and Power Tracking on a Switched FES Cycle With an Unknown Electromechanical Delay

Brendon C. Allen, *Member, IEEE*, Kimberly J. Stubbs, *Graduate Student Member, IEEE*, and Warren E. Dixon, *Fellow, IEEE*

***Abstract*— Functional electrical stimulation (FES) is commonly used to facilitate cycling tasks for people with lower-limb movement disorders. In this work, FES and motor controllers are designed to track a desired power and cadence, respectively, and a Lyapunov-based switched systems analysis is performed to guarantee uniformly ultimately bounded power tracking and global exponential cadence tracking for a switched, delayed, nonlinear, and uncertain FES-cycling system. A unique challenge in this problem is that there is an unknown time-varying input delay to produce force, and a different unknown time-varying residual input delay where force is still produced after stimulation is removed. These delays impact the dwell-time conditions that dictate stimulation timing, and if not properly accounted for can lead to undesired effects such as antagonistic muscles exerting force at the same time or potential instabilities. The proposed controllers were validated by experimental analysis of four participants with neurological conditions (NCs) and five able-bodied participants, and yielded average power and cadence tracking errors of 0.01 ± 0.09 W and −0.05 ± 0.65 revolutions per minute (RPM), respectively, for the able-bodied participants and 0.01 ± 1.11 W and −0.07 ± 1.17 RPM, respectively, for the participants with NCs.**

***Index Terms*— Functional electrical stimulation (FES), input delay, Lyapunov methods, power tracking, switched systems.**

I. Introduction

Neurological conditions (NCs) affect millions of people, often resulting in reduced endurance, limb control, or strength, thus impeding activities of daily living, which over time results in secondary health effects, such as diabetes, reduced cardiovascular fitness, osteoporosis, and a predisposition to depression [1], [2]. For those with lower-body movement disorders, a common treatment is the use of functional electrical stimulation (FES) and a motor to perform cycling tasks, which has been shown to induce numerous health benefits [3], [4].

Closed-loop control of a FES cycle is challenging because of nonlinearities, uncertainties, time-varying dynamics (e.g., disturbances, muscle activation dynamics, etc.), a reduction of FES efficiency with fatigue, switched/alternating control between a motor and FES of multiple muscle groups, and there exists a time varying delay, called the electromechanical delay (EMD),[1] between FES input and muscle force output [6]–[8]. Additionally, FES cycling typically has a lower metabolic efficiency than cycling volitionally due to several factors, including fatigue, poor control of each muscle group, or less than optimal stimulation parameters [9]–[11]. Metabolic efficiency during FES cycling can be improved by increasing the power output (PO), such as by implementing a power-tracking controller, which increases the proportion of fatigue-resistant muscle fibers and reverses muscle atrophy, among other benefits [10], [11].

In recent decades, closed-loop controllers have been developed to ensure torque/power tracking[2] during FES cycling to increase the PO. For example, in [12] torque tracking is performed when it is kinematically efficient, in [13] discretized power tracking is achieved, and in [11] and [14]–[17] there is instantaneous power tracking. However, only the author's prior work in [17], which this work is based on, provided compensation for the EMD of the prior torque tracking results.

EMD compensation is critical to prevent instability and decreased efficiency [6], which motivated the recent development of EMD compensating control schemes such as the author's work in [17]–[21] for a FES cycle system and the work in [22] and [23] for a leg extension system. FES cycling, unlike leg extensions, is a coordinated exercise that requires switched control. A consequence is that the contraction delay (i.e., the delay between the start of FES and the onset of muscle force) and residual delay (i.e., the delay between the end of FES and the end of muscle force) must both be considered during FES cycling to yield efficient muscle contractions [17]–[21]. However, with the exception of our work in [17], the prior results for EMD compensation only provided trajectory (i.e., position and/or cadence) tracking and did not have an objective of increasing the PO, which limits health benefits. Furthermore, numerous efforts have been made to compensate for non-FES systems with input delays (cf. [24]–[31]); however, few have considered switched systems (cf. [28]–[31]). No prior work, other than our preliminary work in [17] has compensated for an input delay, including the residual delay, of a switched system with an uncertain, time-varying, and state-dependent control effectiveness, while

Manuscript received 20 January 2022; revised 3 April 2022; accepted 9 May 2022. Date of publication 24 May 2022; date of current version 28 December 2022. This work was supported in part by the National Defense Science and Engineering Graduate Fellowship Program, in part by the Assistant Secretary of Defense for Health Affairs, through the Congressionally Directed Medical Research Program under Award W81XWH1910330, and in part by NSF under Award 1762829. Recommended by Associate Editor A. Behal. *(Corresponding author: Brendon C. Allen.)*

Brendon C. Allen is with the Department of Mechanical Engineering, Auburn University, Auburn, AL 36849 USA (e-mail: bca0027@auburn.edu).

Kimberly J. Stubbs and Warren E. Dixon are with the Department of Mechanical and Aerospace Engineering, University of Florida, Gainesville, FL 32611 USA (e-mail: kimberlyjstubbs@ufl.edu; wdixon@ufl.edu).

Color versions of one or more figures in this article are available at https://doi.org/10.1109/TCST.2022.3174508.

Digital Object Identifier 10.1109/TCST.2022.3174508

[1]In some literature the EMD corresponds to the time latency between the onset of EMG activity and muscle force [5].

[2]Power and torque tracking are synonymous within the scope of this brief.

simultaneously ensuring both position/cadence tracking and power tracking.

Building on our prior work in [17], a dual objective control structure for simultaneous position/cadence and power tracking is developed for an uncertain, nonlinear, switched FES cycle-rider system with an unknown and time-varying EMD. Furthermore, rider asymmetries are accounted for by implementing instantaneous power tracking via a running integral [11]. Compared to our work in [17], this brief includes volitional effort from the participant in the dynamic model and a series of comparative experiments with a statistical analysis and discussion for nine participants, including four with NCs. Similar to [17], the position/cadence objective is regulated by the motor, similar to clinical practice, and the power objective is regulated using FES to increase the PO and ensure participant contribution. However, due to intermittent FES application there exists uncontrolled periods for the power-tracking objective, which requires a dwell-time analysis, which was further complicated by the existence of the EMD. For example, the EMD required the development of an auxiliary signal to inject a delay-free FES input into the closed-loop error system and Lyapunov–Krasovskii (LK) functionals to aid the stability analysis. Uncertainty in the EMD further complicated the mathematical development (FES input terms are delayed by the actual EMD and an estimate of the EMD) and resulted in more complex and conservative gain and dwell-time conditions. Overall, a switched systems Lyapunov-like analysis is provided to develop dwell-time conditions and to ensure uniformly ultimately bounded torque/power tracking and global exponential position/cadence tracking of a delayed and switched FES cycle system.

A series of experiments were conducted on four participants with NCs and five able-bodied participants. Experiments on the able-bodied participants compared the control system developed in this brief to the control system developed in [11], which did not consider the EMD. It was concluded from the experimental results that the presented control system improved the power tracking performance while reducing the control inputs. Furthermore, the experiments on the participants with NCs included volitional effort and further demonstrated the validity of the developed control system.

II. Dynamics

In this work, delayed functions are denoted as

$$h_\tau \triangleq \begin{cases} h(t-\tau(t)), & t-\tau(t) \geq t_0 \\ 0, & t-\tau(t) < t_0 \end{cases} \tag{1}$$

where $t, t_0 \in \mathbb{R}_{\geq 0}$ denote the time and initial time, respectively, and $\tau : \mathbb{R}_{\geq 0} \to \mathbb{S}$ denotes the unknown EMD, where $\mathbb{S} \subset \mathbb{R}$ represents a set of potential EMD values [7]. Note, the EMD is bounded as $\underline{\tau} \leq \tau \leq \overline{\tau}$, where $\underline{\tau}, \overline{\tau} \in \mathbb{R}_{>0}$ are known constants [7]. The nonlinear, switched, uncertain cycle-rider dynamics are [17]–[21][3]

$$\begin{aligned} M(q)\ddot{q} + V(q,\dot{q})\dot{q} + G(q) + P(q,\dot{q}) + b_c\dot{q} + d(t) \\ = \underbrace{B_E u_e(t)}_{\tau_e(t)} + \underbrace{B_M^\tau(q,\dot{q},\tau,t)u_\tau + \tau_{\text{vol}}(t)}_{\tau_m(q,\dot{q},\tau,t)} \end{aligned} \tag{2}$$

[3]For notational brevity, all explicit dependence on time, t, within the terms $q(t)$, $\dot{q}(t)$, $\ddot{q}(t)$, and $\tau(t)$ is suppressed.

where the measured crank angle, measured angular velocity (cadence), and unmeasured acceleration are denoted by $q : \mathbb{R}_{\geq 0} \to \mathcal{Q}$, $\dot{q} : \mathbb{R}_{\geq 0} \to \mathbb{R}$, and $\ddot{q} : \mathbb{R}_{\geq 0} \to \mathbb{R}$, respectively, where $\mathcal{Q} \subseteq \mathbb{R}$ represents the set of potential crank angles. The effects of inertia, centripetal-Coriolis forces, gravity, passive tissue forces (viscoelastic), damping (viscous), and disturbances are represented by $M : \mathcal{Q} \to \mathbb{R}_{>0}$, $V : \mathcal{Q} \times \mathbb{R} \to \mathbb{R}$, $G : \mathcal{Q} \to \mathbb{R}$, $P : \mathcal{Q} \times \mathbb{R} \to \mathbb{R}$, $b_c \in \mathbb{R}_{>0}$, and $d : \mathbb{R}_{\geq 0} \to \mathbb{R}$, respectively.

The motor torque input, lumped motor effectiveness, and implemented motor control input are denoted as $\tau_e : \mathbb{R}_{\geq 0} \to \mathbb{R}$, $B_E \in \mathbb{R}_{>0}$, and $u_e : \mathbb{R}_{\geq 0} \to \mathbb{R}$, respectively, where $B_E \triangleq B_e k_e$ and $B_e, k_e \in \mathbb{R}_{>0}$ represent the known motor effectiveness and a selectable constant, respectively. Note that the current input into the motor is defined as $u_E \triangleq k_e u_e$. The human torque input, volitional effort, lumped muscle effectiveness, implemented FES control input, and delayed FES input are denoted as $\tau_m : \mathcal{Q} \times \mathbb{R} \times \mathbb{S} \times \mathbb{R}_{\geq 0} \to \mathbb{R}$, $\tau_{\text{vol}} : \mathbb{R}_{\geq 0} \to \mathbb{R}$, $B_M^\tau : \mathcal{Q} \times \mathbb{R} \times \mathbb{S} \times \mathbb{R}_{\geq 0} \to \mathbb{R}_{\geq 0}$, $u : \mathbb{R}_{\geq 0} \to \mathbb{R}$, and $u_\tau : \mathbb{S} \times \mathbb{R}_{\geq 0} \to \mathbb{R}$, respectively. Specifically, the lumped muscle effectiveness term is defined as

$$B_M^\tau(q,\dot{q},\tau,t) \triangleq \sum_{m \in \mathcal{M}} B_m(q,\dot{q},t) k_m \sigma_{m,\tau} \tag{3}$$

where $k_m \in \mathbb{R}_{>0}$, $B_m : \mathcal{Q} \times \mathbb{R} \times \mathbb{R}_{\geq 0} \to \mathbb{R}_{>0}$, and $\sigma_{m,\tau}$ correspond to the muscle $m \in \mathcal{M}$, and represent a selectable constant, unknown muscle effectiveness, and the delayed FES switching signal, respectively, where the set $\mathcal{M} \triangleq \{LQ, LH, LG, RQ, RH, RG\}$ indicates the left (L) and right (R) quadriceps femoris (Q), hamstrings (H), and gluteal (G) muscle groups. Furthermore, the implemented and delayed stimulation inputs (pulse widths) $\forall m \in \mathcal{M}$ are defined as $u_m \triangleq k_m \sigma_m u$ and $u_{m,\tau} \triangleq k_m \sigma_{m,\tau} u_\tau$, respectively, where $\sigma_{m,\tau}$ indicates if a stimulation pulsewidth of $k_m u_\tau$ was applied to muscle $m \in \mathcal{M}$ at time $t - \tau$. The implemented piecewise right-continuous FES switching signals are denoted as $\sigma_m : \mathcal{Q} \times \mathbb{R} \to \{0, 1\}, \forall m \in \mathcal{M}$, and defined as

$$\sigma_m(q,\dot{q}) \triangleq \begin{cases} 1, & q_\alpha(q,\dot{q}) \in \mathcal{Q}_m \\ 1, & q_\beta(q,\dot{q}) \in \mathcal{Q}_m \quad \forall m \in \mathcal{M} \\ 0, & \text{otherwise} \end{cases} \tag{4}$$

where $\mathcal{Q}_m \subset \mathcal{Q}$ denotes the set of crank angles where a contraction in muscle $m \in \mathcal{M}$ would efficiently contribute to positive crank motion (i.e., forward pedaling), and is defined using the definition in [8] as

$$\mathcal{Q}_m \triangleq \{q \in \mathcal{Q} \mid T_m(q) > \varepsilon_m\} \ \forall m \in \mathcal{M} \tag{5}$$

where for muscle $m \in \mathcal{M}$, $\varepsilon_m \in \mathbb{R}_{>0}$, and $T_m : \mathcal{Q} \to \mathbb{R}$ represent a selectable lower threshold and a torque transfer ratio, respectively. The desired muscle contraction regions and kinematic deadzones are defined as $\mathcal{Q}_{\text{FES}} \triangleq \bigcup_{m \in \mathcal{M}} \{\mathcal{Q}_m\}$ and $\mathcal{Q}_{\text{KDZ}} \triangleq \mathcal{Q} \setminus \mathcal{Q}_{\text{FES}}$, respectively. The trigger conditions, denoted by $q_\alpha, q_\beta : \mathcal{Q} \times \mathbb{R} \to \mathbb{R}$, use the upper and lower bounds on the EMD, respectively, to activate/deactivate stimulation for each muscle group to mitigate contractions in antagonistic muscles and to ensure muscle contractions occur over the entire region $\mathcal{Q}_{\text{FES}}$.

The cycle-rider dynamics in (2) have the following properties, which are used to bound unknown parameters in the subsequent analysis [8].

Property 1: The unknown parameters can be bounded as $c_m \leq M \leq c_M$, $|V| \leq c_V|\dot{q}|$, $|G| \leq c_G$, $|P| \leq c_{P_1} + c_{P_2}|\dot{q}|$, $b_c\dot{q} \leq c_c|\dot{q}|$, $|d| \leq c_d$, and $|\tau_{\text{vol}}| \leq c_{vol}$, where $c_m, c_M, c_V, c_G, c_{P_1}, c_{P_2}, c_c, c_d, c_{\text{vol}} \in \mathbb{R}_{>0}$ are known constants.

Property 2: The scaled time derivative of M and V are skew symmetric, $\frac{1}{2}\dot{M} = V$.

Property 3: When $\sum_{m\in\mathcal{M}} \sigma_{m,\tau} > 0$, the FES control effectiveness is bounded as $c_b \leq B_M^\tau \leq c_B$, where $c_b, c_B \in \mathbb{R}_{>0}$ are known constants. Otherwise, $B_M^\tau = 0$.

Property 4: The EMD estimate error, defined as $\tilde{\tau} \triangleq \hat{\tau} - \tau$, is bounded such that $|\tilde{\tau}| \leq \overline{\tilde{\tau}}$, where $\overline{\tilde{\tau}}, \hat{\tau} \in \mathbb{R}_{>0}$ denotes a known constant and a constant estimate of the EMD, respectively.

Assumption 1: Similar to [11], an active estimate of τ_m, denoted by $\hat{\tau}_m : \mathbb{R}_{\geq 0} \to \mathbb{R}$, can be developed (refer to Section V) such that

$$\tilde{\tau}_m \triangleq \hat{\tau}_m - \tau_m \tag{6}$$

where $\tilde{\tau}_m : \mathbb{R}_{\geq 0} \to \mathbb{R}$ denotes the bounded estimation error (i.e., $|\tilde{\tau}_m| \leq c_{\text{est}}$, where $c_{\text{est}} \in \mathbb{R}_{\geq 0}$ is known).

III. Control Development

A. Position/Cadence Error System

The position-tracking error, $e_1 : \mathbb{R}_{\geq 0} \to \mathbb{R}$, is defined as[4]

$$e_1 \triangleq q_d - q \tag{7}$$

where $q_d : \mathbb{R}_{\geq 0} \to \mathbb{R}$ denotes the smooth and bounded desired position (i.e., $q_d, \dot{q}_d, \ddot{q}_d \in \mathcal{L}_\infty$). To aid the subsequent stability analysis, an auxiliary error $e_2 : \mathbb{R}_{\geq 0} \to \mathbb{R}$ is defined as

$$e_2 \triangleq \dot{e}_1 + \alpha_1 e_1 \tag{8}$$

where $\dot{e}_1 \triangleq \dot{q}_d - \dot{q}$ quantifies the cadence-tracking objective, and $\alpha_1 \in \mathbb{R}_{\geq 0}$ denotes a selectable constant. The open-loop position/cadence error system is obtained by taking the time derivative of (8), multiplying by M, adding and subtracting e_1, and using (2), (7), and (8) to yield

$$M\dot{e}_2 = \chi_1 - e_1 - Ve_2 - \tau_m - B_E u_e \tag{9}$$

where $\chi_1 \triangleq M(\ddot{q}_d + \alpha_1\dot{e}_1) + V(\dot{q}_d + \alpha_1 e_1) + G + P + b_c\dot{q} + d + e_1$. Based on (9) and the stability analysis, the motor controller is designed as

$$u_e = \frac{1}{B_E}\left(k_1 e_2 + \left(k_2 + k_3\|y\| + k_4\|y\|^2\right)\text{sgn}(e_2) - \hat{\tau}_m\right) \tag{10}$$

where $y \triangleq [\, e_1 \; e_2 \,]^T$, $\text{sgn}(\cdot)$ represents the signum function, and $k_1, k_2, k_3, k_4 \in \mathbb{R}_{>0}$ are selectable constants. Substituting (10) into (9) and using (6) yields the closed-loop position/cadence error system

$$\begin{aligned} M\dot{e}_2 = \chi - e_1 - Ve_2 - k_1 e_2 \\ -\left(k_2 + k_3\|y\| + k_4\|y\|^2\right)\text{sgn}(e_2) \end{aligned} \tag{11}$$

where $\chi \triangleq \chi_1 + \tilde{\tau}_m$, which can be bounded by Property 1 as

$$|\chi| \leq c_1 + c_2\|y\| + c_3\|y\|^2 \tag{12}$$

where $c_1, c_2, c_3 \in \mathbb{R}_{>0}$ are known constants.

B. Torque Error System

The integral torque error, $e_3 : \mathbb{R}_{\geq 0} \to \mathbb{R}$, is defined as [32]

$$e_3 \triangleq \int_{t_0}^{t} \left(\tau_{m,d}(\theta) - \hat{\tau}_m(\theta)\right) d\theta \tag{13}$$

where $\tau_{m,d} : \mathbb{R}_{\geq 0} \to \mathbb{R}$ is the bounded desired torque (i.e., $\tau_{m,d} \in \mathcal{L}_\infty$). Applying Leibniz's Rule to take the time derivative of (13) yields the torque tracking error

$$\dot{e}_3 = \tau_{m,d}(t) - \hat{\tau}_m(t). \tag{14}$$

The form of (13) is used to enable the FES controller to influence (14), and thus, the subsequently designed torque error system [32]. An auxiliary signal, $e_4 : \mathbb{R}_{\geq 0} \to \mathbb{R}$, is designed as

$$e_4 \triangleq -\int_{t-\hat{\tau}}^{t} u(\theta) d\theta \tag{15}$$

to provide delay compensation by injecting a delay free FES input into the closed-loop error system. To facilitate the subsequent stability analysis, an auxiliary torque error, $r : \mathbb{R} \times \mathbb{R} \to \mathbb{R}$, is defined as

$$r \triangleq \alpha_2 e_3 + \alpha_3 e_4 \tag{16}$$

where $\alpha_2, \alpha_3 \in \mathbb{R}_{>0}$ are selectable constants.

The open-loop torque error system is obtained by taking a time derivative of (16), adding and subtracting $\alpha_2 B_M^\tau u_{\hat{\tau}}$, substituting in (6), and using $\tau_m = B_M^\tau u_\tau + \tau_{\text{vol}}$ to yield

$$\dot{r} = \alpha_2\chi_2 + \alpha_2 B_M^\tau(u_{\hat{\tau}} - u_\tau) - \alpha_3 u + \left(\alpha_3 - \alpha_2 B_M^\tau\right)u_{\hat{\tau}} \tag{17}$$

where $\chi_2 \triangleq \tau_{m,d} - \tau_{\text{vol}} - \tilde{\tau}_m$, which can be bounded using Property 1 and Assumption 1 as $|\chi_2| \leq c_4$, where $c_4 \in \mathbb{R}_{>0}$ is known. Based on (17) and the stability analysis, the FES controller is defined as

$$u = k_s r \tag{18}$$

where $k_s \in \mathbb{R}_{>0}$ is a selectable constant. Due to the form of (13), the FES controller cannot be applied before t_0. The closed-loop torque error system is obtained by substituting (18) into (17) to yield

$$\dot{r} = \alpha_2\chi_2 + \alpha_2 k_s B_M^\tau(r_{\hat{\tau}} - r_\tau) - \alpha_3 k_s r + \left(\alpha_3 - \alpha_2 B_M^\tau\right)k_s r_{\hat{\tau}}. \tag{19}$$

Furthermore, the subsequent analysis is facilitated by defining LK functionals, $Q_1, Q_2 : \mathbb{R}_{\geq 0} \to \mathbb{R}_{\geq 0}$, as

$$Q_1 \triangleq \frac{1}{2}(\alpha_3 - c_b\alpha_2 + \varepsilon_1\omega_1)k_s \int_{t-\hat{\tau}}^{t} r(\theta)^2 d\theta \tag{20}$$

$$Q_2 \triangleq \frac{\omega_2 k_s}{\hat{\tau}} \int_{t-\hat{\tau}}^{t} \int_{s}^{t} r(\theta)^2 d\theta ds \tag{21}$$

where $\varepsilon_1, \omega_1, \omega_2 \in \mathbb{R}_{>0}$ are selectable constants.

[4]Hereafter, for notational brevity, all functional dependencies are suppressed unless required for clarity of exposition.

IV. Stability Analysis

Due to intermittent FES application, the cases when the muscles are active ($B_M^\tau > 0$) and inactive ($B_M^\tau = 0$) must be analyzed along with a consideration of the switching between cases. A common Lyapunov function candidate is used in Theorem 1 to establish the decay rate (when $B_M^\tau > 0$), growth rate (when $B_M^\tau = 0$), and overall boundedness for the torque error system. In Theorem 2, the position and cadence errors are proven to be globally exponentially stable, and the motor controller is shown to be bounded. Define the continuously differentiable, positive-definite Lyapunov function candidates, $V_1 : \mathbb{R} \times \mathbb{R} \times \mathbb{R}_{\geq 0} \times \mathbb{R}_{\geq 0} \to \mathbb{R}_{\geq 0}$ and $V_2 : \mathbb{R} \times \mathbb{R} \to \mathbb{R}_{\geq 0}$, as

$$V_1 \triangleq \frac{1}{2}r^2 + \frac{1}{2}\omega_1 e_4^2 + Q_1 + Q_2 \tag{22}$$

$$V_2 \triangleq \frac{1}{2}e_1^2 + \frac{1}{2}Me_2^2 \tag{23}$$

which can be bounded as

$$\lambda_1\|z\|^2 \leq V_1 \leq \lambda_2\|z\|^2 \tag{24}$$

$$\beta_1\|y\|^2 \leq V_2 \leq \beta_2\|y\|^2 \tag{25}$$

where $\lambda_1 \triangleq \min((1/2), (\omega_1/2))$, $\lambda_2 \triangleq \max(1, (\omega_1/2))$, $\beta_1 \triangleq \min((1/2), (c_m/2))$, $\beta_2 \triangleq \max((1/2), (c_M/2))$, and $z \in \mathbb{R}^4$ is defined as

$$z \triangleq \left[\, r \;\, e_4 \;\, \sqrt{Q_1} \;\, \sqrt{Q_2}\,\right]^T \tag{26}$$

and y is defined following (10).

To aid the analysis in Theorem 1, let $\delta_1, \delta_2, \lambda, \lambda_3, \lambda_4, \upsilon, \upsilon_1, \upsilon_2 \in \mathbb{R}_{>0}$ denote known auxiliary constants, let the switching instances be denoted as $\{t_n^i\}$, $i \in \{m, e\}, n \in \{1, 2, \ldots, \}$, where t_n^m and t_n^e denote the unknown time instances when B_M^τ becomes nonzero and zero for the nth time, respectively, and let $\Delta t_{\min}^m, \Delta t_{\max}^e \in \mathbb{R}_{>0}$ denote the minimum allowable dwell-time for FES-induced muscle contractions, and the maximum allowable dwell-time for no FES-induced contractions, respectively. Furthermore, define $t_0^e \triangleq t_0$ since it is known that FES forces are not present at t_0 (i.e., $B_M^\tau = 0$ initially) due to the FES controller not being applied before t_0. To aid the dwell-time analysis in Theorem 1, define $\{t_j^i\}$, $i \in \{\text{FES}, \text{KDZ}\}$, j $\in \{1, 2, \ldots, \}$, where t_j^{FES} and t_j^{KDZ} denote the known time instants when the crank enters $\mathcal{Q}_{\text{FES}}$ and $\mathcal{Q}_{\text{KDZ}}$ for the jth time, respectively, and recall that (4) was designed to ensure that muscle contractions occur over the entire region $\mathcal{Q}_{\text{FES}}$. Achievable dwell-times can now be defined as

$$\Delta t_{\min}^m \triangleq \min\left(t_j^{\text{KDZ}} - t_j^{\text{FES}}\right)\ \forall j \tag{27}$$

$$\Delta t_{\max}^e \triangleq \max\left(t_{j+1}^{\text{FES}} - t_j^{\text{KDZ}}\right)\ \forall j \tag{28}$$

where $\Delta t_{\min}^m$ and $\Delta t_{\max}^e$ are dictated by a minimum and maximum allowable cadence after $\mathcal{Q}_{\text{FES}}$ has been defined.

Theorem 1: For the closed-loop torque error system in (19) and the definition of z in (26), the FES controller in (18) yields bounded torque tracking when $B_M^\tau > 0$ *(i.e., FES forces are present) in the sense that*

$$\|z(t)\|^2 \leq \frac{\lambda_2}{\lambda_1}\left\|z\left(t_n^m\right)\right\|^2 \exp\left(-\lambda_3\left(t - t_n^m\right)\right) + \frac{\upsilon_1}{\lambda_1\lambda_3}\left(1 - \exp\left(-\lambda_3\left(t - t_n^m\right)\right)\right). \tag{29}$$

$\forall t \in [t_n^m, t_n^e)$, $\forall n \in \{1, 2, \ldots, \}$*, bounded torque tracking when* $B_M^\tau = 0$ *(i.e., FES forces are not present) in the sense that*

$$\|z(t)\|^2 \leq \frac{\lambda_2}{\lambda_1}\left\|z\left(t_n^e\right)\right\|^2 \exp\left(\lambda_4\left(t - t_n^e\right)\right) - \frac{\upsilon_2}{\lambda_1\lambda_4}\left(1 - \exp\left(\lambda_4\left(t - t_n^e\right)\right)\right). \tag{30}$$

$\forall t \in [t_n^e, t_{n+1}^m)$, $\forall n \in \{0, 1, 2, \ldots, \}$*, and overall uniformly ultimately bounded torque tracking in the sense that* $\limsup_{t\to\infty} \|z(t)\| < (\gamma^2 - \delta)^{1/2}$*, where* $\delta \in (0, \gamma^2)$ *is a known constant, provided that Assumption 1 and the subsequent gain/initial conditions are satisfied*[5]

$$\alpha_3 \geq c_B\alpha_2, \qquad \omega_2 \geq \frac{3\hat{\tau}^2\omega_1 k_s^2}{\varepsilon_1}, \qquad \alpha_3 k_s \hat{\tau} < 1 \tag{31}$$

$$\overline{\overline{\tau}} \leq \frac{1}{k_s^2\alpha_2^2 c_B^2}(4c_b\alpha_2 - 2\alpha_3 - 4\varepsilon_1\omega_1 - 4\omega_2) \tag{32}$$

$$\lambda_3\Delta t_{\min}^m > \lambda_4\Delta t_{\max}^e \tag{33}$$

$$\frac{\upsilon}{1 - \exp(-\lambda)} < \lambda_1\gamma^2 \tag{34}$$

$$\lambda_2\|z(t_0)\|^2 \exp\left(\lambda_4\Delta t_{max}^e\right) + \frac{\upsilon_2}{\lambda_4}\left(\exp\left(\lambda_4\Delta t_{max}^e\right) - 1\right) < \lambda_1\gamma^2. \tag{35}$$

Proof: Available upon request. ■

Theorem 2 is now provided to establish the decay rate for the position and cadence error system for all time.

Theorem 2: For the closed-loop position/cadence error system in (11) and the definition of y following (10), the motor controller in (10) yields global exponential position/cadence tracking in the sense that

$$\|y(t)\| \leq \sqrt{\frac{\beta_2}{\beta_1}}\|y(t_0)\| \exp\left(-\frac{\min(\alpha_1, k_1)}{2\beta_2}(t - t_0)\right). \tag{36}$$

$\forall t \in [t_0, \infty)$*, provided the following gain conditions are satisfied*:

$$k_2 \geq c_1,\ k_3 \geq c_2,\ k_4 \geq c_3 \tag{37}$$

where c_1, c_2, *and* c_3 *are introduced in (12).*

Proof: Available upon request. ■

V. Experiment

Henceforth, the combined efforts of the developed controllers in (10) and (18) will be labeled as Controller A, the control structure developed in [11] (which assumed that the EMD was negligible) will be labeled as Controller B, and the developed motor controller in (10) alone will be labeled as Controller C. Controllers A and B have the same form (i.e., the motor tracks the position/cadence and the FES tracks the power); however, Controller A provides compensation for the EMD.

[5] Note that from (1) and the fact that each term in $\|z\|$ is a time-based integral [see (13), (15), (16), (20), (21), and (26)], it can be seen that $\|z(t_0)\| = 0$ by definition. Therefore, (35) can be reduced to the following gain condition: $(\upsilon_2/\lambda_4)(\exp(\lambda_4\Delta t_{max}^e) - 1) < \lambda_1\gamma^2$.

A. Experimental Testbed

The experimental testbed consisted of the modified stationary TerraTrike Rover recumbent tricycle presented in [11, Sec. 5.1].

B. Experimental Methods

Comparative experiments were performed on three male and two female able-bodied participants (ages 25.0 ± 2.8 years), henceforth labeled S1–S5, and two male and female participants (ages 44.3 ± 13.5 years), henceforth labeled N1 to N4. Participant N1 has Spina Bifida, Participants N2 and N3 have Multiple Sclerosis, and Participant N4 has Cerebral Palsy. Prior to participation, written informed consent approved by the UF Institutional Review Board (IRB201600881) was provided. Experiments were either performed with or without volitional contributions by the participant, which are subsequently called active and passive therapy experiments, respectively. During the passive therapy experiments, the participants were blind to the actual/desired trajectories and were instructed to remain passive to simulate a situation where a participant is unable to provide voluntary contribution (e.g., due to muscle weakness or paralysis). During the active therapy experiments, the participants were shown a real-time plot of $e_3(t)$, exclusively, and were instructed to contribute to the best of their ability to the control objective, and FES was applied as required.

Prior to performing an experiment, Axelgaard ValuTrode CF7515 electrodes were placed over each muscle group (i.e., quadriceps, gluteal, and hamstrings) of a participant seated with their feet secured to the cycle using Össur Rebound Air Tall orthotic boots. A FES comfort limit was obtained for each muscle group by running the cycle at 50 revolutions per minute (RPM) and then applying and modulating open-loop stimulation, to one muscle group at a time, until the participant's comfort limit was determined for each muscle. Subsequently, the stimulation input to a given muscle was saturated if it exceeded the participant's comfort limit for that muscle.

A preliminary experiment was performed to estimate the passive torques of the cycle and rider about the crank [i.e., the terms on the left-hand side of (2)] denoted by $\hat{\tau}_{\text{pas}}$. During this trial, FES was not applied and the rider was instructed to not provide volitional effort. The trial consisted of using the motor controller in (10) to run the cycle at 50 RPM (the desired cadence) while simultaneously recording the angular position and torque/power. An eighth-order Fourier fit was then applied to the recorded torque and position data to obtain $\hat{\tau}_{\text{pas}}$. An active estimate of $\hat{\tau}_m$ could then be obtained by subtracting $\hat{\tau}_{\text{pas}}$ from the active torque sensor measurements, which satisfies Assumption 1.

The experimental protocol consisted of the motor controller associated with either Controller A, B, or C tracking a desired cadence that increased from 0 to 50 RPM over the first 30 s and then tracking 50 RPM for the remaining 90 s of the experiment (the steady-state portion of the experiment). After the cadence increase (i.e., $t = 30$ s), the corresponding FES controller was activated to track the desired power trajectory, denoted by $P_d : \mathbb{R}_{\geq 0} \to \mathbb{R}$ and defined as $P_d \triangleq \tau_{m,d}\dot{q}_d$, which smoothly increased from 0 to the desired power (1 and 5 W for passive and active therapy experiments, respectively) and thereafter was held constant. Furthermore, the measured torque can be converted to the measured power, $P : \mathbb{R}_{\geq 0} \to \mathbb{R}$, by using $P \triangleq \hat{\tau}_m \dot{q}$. Passive therapy experiments (i.e., no volition) were performed on the able-bodied participants by implementing Controllers A and B in a random order. Active therapy experiments (i.e., with volition) were performed on the participants with NCs by implementing Controllers A and C in a random order. Prior to the experiments, up to two tests were performed for each controller where the controller gains were adjusted using an empirical-based method. Note, the gain conditions in (31)–(35) are sufficient conditions to stabilize the system; however, in practice the gain conditions provide a starting point and subsequently can be adjusted to achieve desired performance. No practice was permitted for the able-bodied participants; however, the participants with NCs were permitted one practice run per controller since they provided volition. Rest of 3 to 5 min was provided between each experiment. Subsequently, experiments are referred to as the participant number followed by the letter of the controller; for example, S1A denotes the experiment for participant S1 using Controller A.

VI. Results

A. Results From Able-Bodied Participants

To validate Controller A, passive therapy experiments were performed on the able-bodied participants using Controllers A and B. The root mean square (RMS) and peak tracking (i.e., cadence and power) errors in addition to the required motor and FES effort are summarized in Table I for the able-bodied participants. The tracking (i.e., cadence and power) performance and control inputs (i.e., motor and FES) for participant S1, which depict a typical result, are provided in Fig. 1 for Controllers A and B and in Fig. 2 for Controller A. Furthermore, across the able-bodied participants, Controllers A and B produced an average cadence error of −0.05 ± 0.65 and −0.05 ± 0.73 RPM, respectively, an average integral torque error of 0.34 ± 0.08 and 1.13 ± 0.76 Nms, respectively, and an average power error ($\dot{e}_3$) of 0.01 ± 0.09 and 0.38 ± 0.18 W, respectively.

1) Statistical Analysis and Discussion: To compare the performance of Controllers A and B, paired difference statistical tests were implemented, using the data for participants S1–S5 in Table I, on the peak and RMS cadence ($\dot{e}_1$), integral torque (e_3), and power tracking errors ($\dot{e}_3$), in addition to the average FES and motor effort, and the standard deviation of the FES and motor effort. Normality of the paired difference data for each measurement was confirmed using Shapiro–Wilk's normality test. One-sided paired t-tests were implemented to determine that the RMS (P-Value = 0.038) and peak (P-Value = 0.035) integral torque errors, RMS (P-Value = 0.022) and peak (P-Value = 0.002) power errors, and the average motor (P-Value = 0.008) and FES (P-Value = 0.031) effort were significantly larger for Controller B when compared to

TABLE I

COMPARATIVE RESULTS FOR THE EACH PARTICIPANT DURING STEADY STATE*,†

Controller	Participant	RMS Error $\dot{e}_1$ (RPM)	Peak Error $\dot{e}_1$ (RPM)	RMS Error e_3 (Nms)	Peak Error e_3 (Nms)	RMS Error $\dot{e}_3$ (W)‡	Peak Error $\dot{e}_3$ (W)‡	Motor Effort (A)‖	FES Effort (μs)#
A	S1	0.75	2.40	0.57	0.80	0.13	0.44	1.51±0.84	103.96±16.83
	S2	0.58	2.09	0.48	0.74	0.07	0.41	1.49±0.67	54.03±5.74
	S3	0.67	2.51	0.32	0.49	0.09	0.31	1.22±0.69	54.48±5.35
	S4	0.63	2.39	0.22	0.31	0.05	0.18	1.38±0.72	67.00±5.21
	S5	0.65	2.54	0.20	0.41	0.09	0.29	1.27±0.70	45.86±8.96
	Average	**0.66**	**2.38**	**0.36**	**0.55**	**0.09**	**0.32**	**1.37±0.73**	**65.07±8.42**
B	S1	0.74	2.57	2.56	4.92	0.43	0.86	1.61±0.81	123.17±17.33
	S2	0.72	2.31	1.73	3.48	0.77	0.96	1.65±0.82	61.49±8.63
	S3	0.89	2.99	0.13	0.32	0.27	0.83	1.44±0.77	67.82±10.78
	S4	0.64	1.95	1.99	3.86	0.79	1.02	1.55±0.74	72.40±16.24
	S5	0.68	2.42	0.45	0.73	0.16	0.58	1.30±0.73	44.89±7.02
	Average	**0.73**	**2.45**	**1.37**	**2.66**	**0.48**	**0.85**	**1.51±0.78**	**73.95±12.00**
A	N1	1.34	4.88	0.22	0.83	0.60	2.71	1.39±1.07	46.53±3.90
	N2	1.15	4.53	1.12	4.70	1.79	5.89	1.55±0.99	31.22±1.61
	N3	1.13	4.48	0.44	1.64	1.33	4.06	1.53±1.01	51.84±10.48
	N4	1.06	4.43	0.28	1.12	0.72	3.15	1.35±1.03	27.03±4.41
	Average	**1.17**	**4.58**	**0.52**	**2.07**	**1.11**	**3.95**	**1.45±1.02**	**39.15±5.10**
C	N1	1.18	4.76	0.41	1.58	0.90	4.97	1.22±0.85	0.00±0.00
	N2	0.93	3.79	3.20	7.95	3.03	7.28	1.22±0.78	0.00±0.00
	N3	1.17	4.58	1.00	4.64	1.26	7.80	1.48±0.98	0.00±0.00
	N4	1.42	7.33	2.23	7.04	2.64	10.13	1.54±1.23	0.00±0.00
	Average	**1.18**	**5.11**	**1.71**	**5.30**	**1.96**	**7.54**	**1.36±0.96**	**0.00±0.00**

*For each participant, the desired cadence was set to 50 RPM. For participants S1-S5, no volition was provided and the desired power was set to 1 W. For participants N1-N4, volition was provided and the desired power was set to 5 W.

†RMS error denotes the root mean square error and peak error denotes the maximum absolute value of the error over the entire experimental run.

‡For post-processing, a two crank cycle (i.e., a moving window of 2.4s) averaging filter was applied.

‖The average ± standard deviation of $|u_E|$, where u_E denotes the current input to the motor.

#The average ± standard deviation of the maximum stimulation delivered to each muscle group during each FES region.

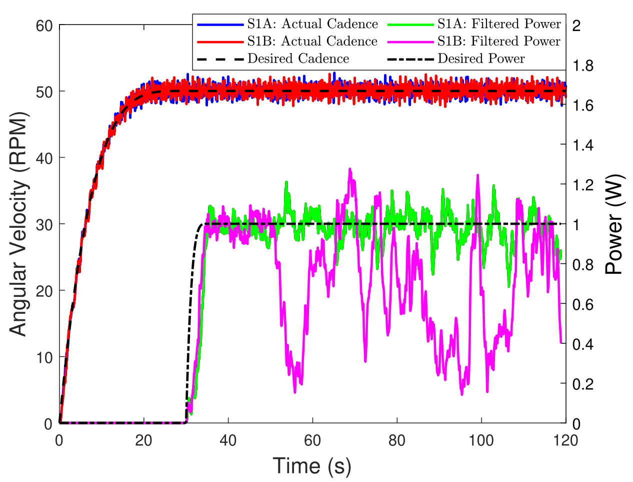

Fig. 1. S1A and S1B: The desired versus the actual cadence and filtered power. For visual clarity, a two crank cycle (i.e., a moving window of 2.4 s) averaging filter was applied to the power.

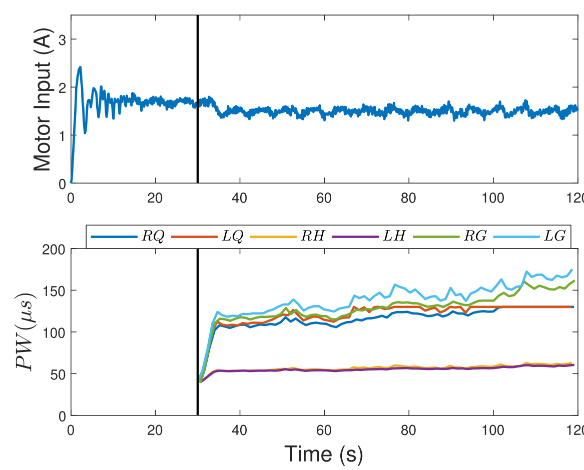

Fig. 2. S1A: The filtered motor input using a 1.2-s moving average filter (top); and the maximum stimulation applied to the right (R) and left (L) quadriceps (Q), hamstring (H), and gluteal (G) for each FES region (bottom). Steady-state is indicated by the vertical black line. The flat portion of the FES input into the LQ is a result of saturating the input for rider comfort.

Controller A. However, no significant effect was determined between Controllers A and B for the RMS (P-Value = 0.072) and peak (P-Value = 0.357) cadence errors or the motor (P-Value = 0.074) and FES (P-Value = 0.092) standard deviations.

From inspection of Fig. 1, Controller A improved the torque/power tracking performance for participant S1, whereas the cadence tracking performance is essentially unaffected, which is consistent with the conclusions of the statistical analysis. However, in Fig. 1 the power tracking appears to steadily worsen with time for Controller A, likely as a result of fatigue. Examining the corresponding control inputs in Fig. 2 confirms that, prior to saturation, the FES inputs tended to increase with time, which is indicative of the participant

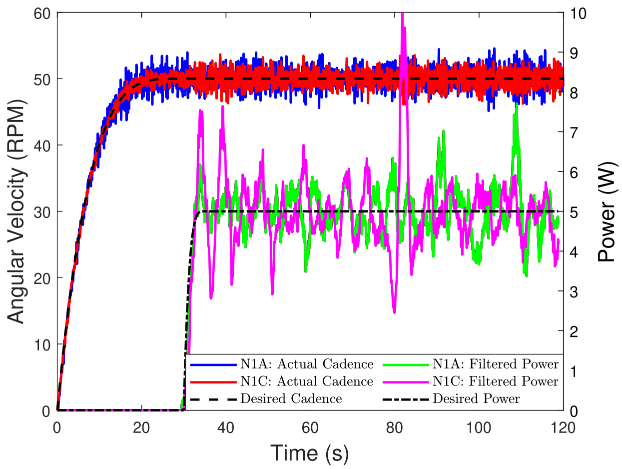

Fig. 3. N1A and N1C: The desired versus the actual cadence and filtered power. For visual clarity, a two crank cycle (i.e., a moving window of 2.4 s) averaging filter was applied to the power.

beginning to fatigue. Although not depicted, it should be noted that the FES inputs for Controller B tended to rapidly saturate for each participant, which likely resulted in Controller B's poor power tracking performance. Overall, it can be concluded that relative to Controller B, Controller A improved the torque/power tracking performance while requiring both a smaller average FES and motor effort.

B. Results From Participants With NCs

Since Controller A improved the power/torque tracking and decreased the required control inputs, Controller B was not implemented on the participants with NCs. Recall that active therapy (i.e., with volitional effort) experiments were performed on the participants with NCs, therefore Controller C was implemented to determine how well the participant could track the desired power on their own volition. The results of the experiments using Controllers A and C on the participants with NCs are included in Table I. A plot of the cadence and power-tracking results for participant N1, which represent a typical result, are included in Fig. 3 for Controllers A and C. Furthermore, across the participants with NCs, Controllers A and C produced an average integral torque error of 0.23 ± 0.44 and 0.64 ± 1.57 Nms, respectively, an average power error ($\dot{e}_3$) of 0.01 ± 1.11 and 0.01 ± 1.95 W, respectively, and an average cadence error of -0.07 ± 1.17 RPM for both controllers.

1) Statistical Analysis and Discussion: Statistical tests (i.e., Shapiro–Wilk and one-sided paired t-tests) were conducted, using the data for participants N1–N4 in Table I, to conclude normality and that the RMS (P-Value $= 0.045$) and peak (P-Value $= 0.028$) integral torque error, and the peak power error (P-Value $= 0.03$) were significantly larger for Controller C when compared to Controller A. Likewise, no significant effect was determined between Controllers A and C for the RMS (P-Value $= 0.487$) or peak (P-Value $= 0.278$) cadence error, the RMS power error (P-Value $= 0.080$), the average motor input (P-Value $= 0.230$), or the motor effort standard deviation (P-Value $= 0.279$).

From the statistical analysis and by inspection of Fig. 3, the torque/power tracking performance was improved when the FES controller from Controller A was implemented compared to Controller C, which provided no torque tracking assistance. The results in Table I and the statistical results demonstrate both the power and cadence tracking ability of Controller A, despite the uncertainties and time-varying nature associated with the rider-cycle system, including the wide-range of conditions of each participant, in addition to the effects of fatigue, the EMD, and volitional efforts. Overall, Controller A has proven its capability of achieving both cadence and power tracking for both passive and active therapy experiments on participants with and without NCs.

VII. Conclusion

In an effort to improve rehabilitation, a dual objective control system is developed to track both PO and cadence using FES and motor controllers, respectively. The torque/power is tracked in real-time by implementing a running integral of the torque tracking error. EMD compensation was provided by developing trigger conditions to properly time stimulation, LK functionals, and an auxiliary tracking error that injected a delay-free stimulation input into the closed-loop error system. A Lyapunov-like switched system analysis was performed to ensure exponential power tracking to an ultimate bound and global exponential cadence tracking for the uncertain, nonlinear, switched, and delayed cycle-rider system that was subject to uncertain disturbances such as an unknown volitional effort. A series of comparative experiments were performed on nine participants, including four with a variety of NCs, to validate the developed FES and motor controllers. Future efforts will focus on developing methods to reduce the rate of fatigue caused by FES, such as developing adaptive torque tracking controllers to provide more efficient closed-loop stimulation.

Acknowledgment

Any opinions, findings, and conclusions, or recommendations expressed in this material are those of the author(s) and do not necessarily reflect the views of the sponsoring agency.

References

[1] J. H. Rimmer and J. L. Rowland, “Health promotion for people with disabilities: Implications for empowering the person and promoting disability-friendly environments,” *Amer. J. Lifestyle Med.*, vol. 2, no. 5, pp. 409–420, Sep. 2008.

[2] D. Newham and N. D. N. Donaldson, “FES cycling,” in *Operative Neuromodulation*. Vienna, Austria: Springer, 2007, pp. 395–402.

[3] C.-W. Peng *et al.*, “Review: Clinical benefits of functional electrical stimulation cycling exercise for subjects with central neurological impairments,” *J. Med. Biol. Eng.*, vol. 31, no. 1, pp. 1–11, 2011.

[4] A. T. Harrington, C. G. A. McRae, and S. C. K. Lee, “Evaluation of functional electrical stimulation to assist cycling in four adolescents with spastic cerebral palsy,” *J. Pediatrics*, vol. 2012, pp. 1–11, Jan. 2012.

[5] A. Nordez, T. Gallot, S. Catheline, A. Guével, C. Cornu, and F. Hug, “Electromechanical delay revisited using very high frame rate ultrasound,” *J. Appl. Physiol.*, vol. 106, no. 6, pp. 1970–1975, Jun. 2009.

[6] R. J. Downey, M. Merad, E. J. Gonzalez, and W. E. Dixon, “The time-varying nature of electromechanical delay and muscle control effectiveness in response to stimulation-induced fatigue,” *IEEE Trans. Neural Syst. Rehabil. Eng.*, vol. 25, no. 9, pp. 1397–1408, Sep. 2017.

[7] B. C. Allen, K. J. Stubbs, and W. E. Dixon, “Characterization of the time-varying nature of electromechanical delay during FES-cycling,” *IEEE Trans. Neural Syst. Rehabil. Eng.*, vol. 28, no. 10, pp. 2236–2245, Oct. 2020.

[8] M. J. Bellman, R. J. Downey, A. Parikh, and W. E. Dixon, "Automatic control of cycling induced by functional electrical stimulation with electric motor assistance," *IEEE Trans. Autom. Sci. Eng.*, vol. 14, no. 2, pp. 1225–1234, Apr. 2017.

[9] K. J. Hunt, D. Hosmann, M. Grob, and J. Saengsuwan, "Metabolic efficiency of volitional and electrically stimulated cycling in able-bodied subjects," *Med. Eng. Phys.*, vol. 35, no. 7, pp. 919–925, Jul. 2013.

[10] D. J. Newham and N. de N. Donaldson, "FES cycling," *J. Autom. Control*, vol. 18, no. 2, pp. 73–76, 2008.

[11] C. A. Cousin *et al.*, "Closed-loop cadence and instantaneous power control on a motorized functional electrical stimulation cycle," *IEEE Trans. Control Syst. Technol.*, vol. 28, no. 6, pp. 2276–2291, Nov. 2020.

[12] V. Duenas, C. A. Cousin, V. Ghanbari, E. J. Fox, and W. E. Dixon, "Torque and cadence tracking in functional electrical stimulation induced cycling using passivity-based spatial repetitive learning control," *Automatica*, vol. 115, pp. 1–9, May 2020.

[13] E. Ambrosini, S. Ferrante, T. Schauer, G. Ferrigno, F. Molteni, and A. Pedrocchi, "Design of a symmetry controller for cycling induced by electrical stimulation: Preliminary results on post-acute stroke patients," *Artif. Organs*, vol. 34, no. 8, pp. 663–667, Aug. 2010.

[14] K. J. Hunt *et al.*, "Control strategies for integration of electric motor assist and functional electrical stimulation in paraplegic cycling: Utility for exercise testing and mobile cycling," *IEEE Trans. Neural Syst. Rehabil. Eng.*, vol. 12, no. 1, pp. 89–101, Mar. 2004.

[15] A. Farhoud and A. Erfanian, "Fully automatic control of paraplegic FES pedaling using higher-order sliding mode and fuzzy logic control," *IEEE Trans. Neural Syst. Rehabil. Eng.*, vol. 22, no. 3, pp. 533–542, May 2014.

[16] C. A. Cousin, V. H. Duenas, C. A. Rouse, and W. E. Dixon, "Motorized functional electrical stimulation for torque and cadence tracking: A switched Lyapunov approach," in *Proc. IEEE 56th Annu. Conf. Decis. Control (CDC)*, Dec. 2017, pp. 5900–5905.

[17] B. C. Allen, K. J. Stubbs, and W. E. Dixon, "Robust power and cadence tracking on a motorized FES cycle with an unknown time-varying input delay," in *Proc. 59th IEEE Conf. Decis. Control (CDC)*, Dec. 2020, pp. 3407–3412.

[18] B. C. Allen, C. A. Cousin, C. A. Rouse, and W. E. Dixon, "Robust cadence tracking for switched FES-cycling with an unknown time-varying input delay," *IEEE Trans. Control Syst. Technol.*, vol. 30, no. 2, pp. 827–834, Mar. 2022.

[19] B. C. Allen, K. J. Stubbs, and W. E. Dixon, "Position and cadence tracking of a motorized FES-cycle with an unknown time-varying input delay using saturated FES control," *Automatica*, vol. 139, May 2022, Art. no. 110176.

[20] B. C. Allen, K. J. Stubbs, and W. E. Dixon, "Robust cadence tracking for switched FES-cycling with an unknown time-varying input delay using a time-varying estimate," in *Proc. IFAC World Congr.*, 2020, pp. 10123–10128.

[21] H. M. Sweatland, B. C. Allen, M. L. Greene, and W. E. Dixon, "Deep neural network real-time control of a motorized functional electrical stimulation cycle with an uncertain time-varying electromechanical delay," in *Proc. ASME Int. Mech. Eng. Congr. Expo*, Nov. 2021.

[22] I. Karafyllis, M. Malisoff, M. de Queiroz, M. Krstic, and R. Yang, "Predictor-based tracking for neuromuscular electrical stimulation," *Int. J. Robust Nonlinear Control*, vol. 25, no. 14, pp. 2391–2419, 2015.

[23] S. Obuz, V. H. Duenas, R. J. Downey, J. R. Klotz, and W. E. Dixon, "Closed-loop neuromuscular electrical stimulation method provides robustness to unknown time-varying input delay in muscle dynamics," *IEEE Trans. Control Syst. Technol.*, vol. 28, no. 6, pp. 2482–2489, Nov. 2020.

[24] M. Krstic, *Delay Compensation for Nonlinear, Adaptive, and PDE Systems*. Cham, Switzerland: Springer, 2009.

[25] L. Karafyllis and M. Krstic, *Predictor Feedback for Delay Systems: Implementations Approximations*. Cham, Switzerland: Springer, 2017.

[26] M. Bagheri, P. Naseradinmousavi, and M. Krstić, "Feedback linearization based predictor for time delay control of a high-DOF robot manipulator," *Automatica*, vol. 108, Oct. 2019, Art. no. 108485.

[27] F. Mazenc and M. Malisoff, "Continuous discrete sequential observers for time-varying systems under sampling and input delays," *IEEE Trans. Autom. Control*, vol. 65, no. 4, pp. 1704–1709, Apr. 2020.

[28] F. Mazenc, M. Malisoff, and H. Özbay, "Stability and robustness analysis for switched systems with time-varying delays," *SIAM J. Control Optim.*, vol. 56, no. 1, pp. 158–182, Jan. 2018.

[29] Y.-E. Wang, X.-M. Sun, and F. Mazenc, "Stability of switched nonlinear systems with delay and disturbance," *Automatica*, vol. 69, pp. 78–86, Jul. 2016.

[30] Y.-E. Wang, B. Niu, B.-W. Wu, C. Wu, and X.-J. Xie, "Asynchronous switching for switched nonlinear input delay systems with unstable subsystems," *J. Franklin Inst.*, vol. 355, no. 5, pp. 2912–2931, Mar. 2018.

[31] D. Yang, X. Li, and J. Qiu, "Output tracking control of delayed switched systems via state-dependent switching and dynamic output feedback," *Nonlinear Anal., Hybrid Syst.*, vol. 32, pp. 294–305, 2019.

[32] W. E. Dixon, A. Behal, D. M. Dawson, and S. Nagarkatti, *Nonlinear Control of Engineering Systems: A Lyapunov-Based Approach*. Boston, MA, USA: Birkhäuser, 2003.